Dynamic model with scale-dependent coefficients in the viscous range

By C. Meneveau[1] & T. S. Lund[2]

The standard dynamic procedure is based on the scale-invariance assumption that the model coefficient C is the same at the grid and test-filter levels. In many applications this condition is not met, e.g. when the filter-length, Δ, approaches the Kolmogorov scale, and $C(\Delta \to \eta) \to 0$. Using *a priori* tests, we show that the standard dynamic model yields the coefficient corresponding to the *test-filter* scale ($\alpha\Delta$) instead of the grid-scale (Δ). Several approaches to account for scale dependence are examined and/or tested in large eddy simulation of isotropic turbulence: (a) Take the limit $\alpha \to 1$; (b) Solve for two unknown coefficients $C(\Delta)$ and $C(\alpha\Delta)$ in the least-square-error formulation; (c) The 'bi-dynamic model', in which two test-filters (e.g. at scales 2Δ and 4Δ) are employed to gain additional information on possible scale-dependence of the coefficient, and an improved estimate for the grid-level coefficient is obtained by extrapolation. (d) Use theoretical predictions for the ratio $C(\alpha\Delta)/C(\Delta)$ and dynamically solve for $C(\Delta)$. None of these options is found to be entirely satisfactory, although the last approach appears applicable to the viscous range.

1. Introduction

One of the underlying ideas of the dynamic procedure (Germano *et al.*, 1991) for large eddy simulation (LES) is scale-similarity, which allows information obtained from the resolved field to be utilized for modeling the subgrid scales. Typically, this information consists of a dimensionless model coefficient (e.g. the Smagorinsky coefficient) which is assumed to have the same value at the grid-scale Δ and test-filter scale $\alpha\Delta$, where $\alpha = 2$ in most applications. Concretely, within the context of the Smagorinsky model, the Germano identity leads to

$$L_{ij} = C(\alpha\Delta)A_{ij} - \widehat{C(\Delta)B^*_{ij}}, \tag{1}$$

where $A_{ij} = -2(\alpha\Delta)^2|\hat{\bar{S}}|\hat{\bar{S}}_{ij}$, $B^*_{ij} = -2\Delta^2|\bar{S}|\bar{S}_{ij}$, $|\bar{S}| = \sqrt{2\bar{S}_{ij}\bar{S}_{ij}}$, and $L_{ij} = \widehat{\bar{u}_i\bar{u}_j} - \hat{\bar{u}}_i\hat{\bar{u}}_j$ is the resolved stress. The fundamental scale-similarity assumption of the standard dynamic model is that the model coefficients $C(\Delta) = C(\alpha\Delta) = C$. With this assumption, C is obtained by minimizing the error in Eq. 1 averaged over the independent tensor components (Lilly, 1992) and, if it exists, over a region

1 The Johns Hopkins University
2 Center for Turbulence Research

of statistical homogeneity (Germano *et al.*, 1991; Ghosal *et al.*, 1995). For fully inhomogeneous flows, averaging can be performed over pathlines (Meneveau *et al.*, 1996).

As in other applications, it will be assumed here that the averaging operations sufficiently diminish spatial variations of C, so that one can neglect the error incurred in extracting C from the test-filter operation (see Ghosal *et al.*, 1995). Thus, the second term in the rhs of Eq. (1) is replaced with $C(\Delta)B_{ij}$, where $B_{ij} = \widehat{B^*}_{ij}$. Also, in this work we will examine the dynamic procedure in conjunction with the Smagorinsky model. While other base-models such as similarity models have been proposed (Bardina *et al.*, 1980; Liu *et al.*, 1994), they typically require an additional eddy-viscosity term (mixed model, Bardina 1983; Zang *et al*, 1993; Liu *et al.*, 1995). Thus, it is of interest to continue to examine the Smagorinsky model in parallel to other efforts on improved base models.

Under the assumption of scale-invariance, the dynamic Smagorinsky model yields

$$C = \frac{\langle M_{ij} L_{ij} \rangle}{\langle M_{ij} M_{ij} \rangle}, \tag{2}$$

where

$$M_{ij} = A_{ij} - B_{ij}, \tag{2a}$$

and where $\langle\rangle$ denotes an average over directions of statistical homogeneity or over pathlines.

When applied to the simple problem of either forced or decaying isotropic turbulence at large Reynolds number, the resulting coefficient is typically between $C \simeq 0.02$ and 0.03, independent of Δ. This agrees with the classical result by Lilly (1967) which relates C to the universal Kolmogorov constant c_K according to

$$C = \left(\frac{2}{3c_K}\right)^{3/2} \pi^{-2} \simeq 0.027, \quad \text{for} \quad c_K = 1.6. \tag{3}$$

This result is obtained from balancing the rate of SGS dissipation with the total dissipation, and evaluating moments of the resolved strain-rate tensor by requiring the resolved portion of the flow to display an inertial-range Kolmogorov spectrum. When the filter-scale is within the inertial range, this argument indeed yields a Δ-independent result.

While the above analysis is useful as a guide, it is not generally applicable to LES of complex flows, where the filter (grid) scale Δ may not fall inside a pure inertial range. For instance, in certain parts of the domain, Δ may approach the flow's integral scale, or the flow may be undergoing rapid distortions so that the inertial range is perturbed. In other regions of the flow, the grid scale may approach the viscous scale. In such situations, the coefficient may dependent on Δ, and the assumption $C(\Delta) = C(\alpha\Delta)$ used in the dynamic model is not strictly applicable.

The objective of this study is to examine the dynamic model when the coefficient depends on scale. A convenient application in which to examine this issue

numerically is forced isotropic turbulence, when $\Delta \to \eta$, where η is the Kolmogorov scale. We will study coefficient scale dependence using filtered DNS data (*a priori* test) and perform LES at varying viscosity, so that Δ/η, or the mesh-Reynolds number (McMillan & Ferziger, 1979), defined as $Re_\Delta = \Delta^2|\bar{S}|/\nu$, decreases towards $Re_\Delta \simeq 1$.

First, a review of the expected behavior of $C(\Delta \to \eta)$ is given in §2. In §3, we analyze highly-resolved DNS data at moderate Reynolds number and compare the real Smagorinsky coefficient to that obtained from the dynamic model under the assumption that $C(\Delta) = C(\alpha\Delta)$. The effect of varying α is also examined. In section §4, we report on several attempts to generalize the dynamic model to explicitly take into account the scale-dependence of the coefficient. Conclusions are outlined in §5.

2. Smagorinsky coefficient in the viscous range

Before considering the dynamic Smagorinsky model, it is useful to establish the expected behavior of the Smagorinsky coefficient as the grid-scale approaches the viscous range. The analysis is based on a generalization of the argument by Lilly (1967) and was recently carried out by Voke (1996) who expressed the results in terms of the mesh-Reynolds number Re_Δ. We shall also need results in terms of Δ/η, so the analysis is briefly repeated below. Examination of the equation for resolved kinetic energy in isotropic, statistically steady, and forced (force f_i) turbulence yields

$$\langle f_i \bar{u}_i \rangle = -\langle \tau_{ij} \bar{S}_{ij} \rangle + 2\nu \langle \bar{S}_{ij}^2 \rangle , \tag{4}$$

where $\langle\rangle$ denotes a volume average. The last term above is viscous dissipation of resolved motion, which was neglected in the traditional Lilly (1967) analysis as $\Delta >> \eta$. Using the fact that in steady turbulence the injection rate $\langle f_i \bar{u}_i \rangle$ equals the overall rate of dissipation ϵ, replacing the Smagorinsky model with a possibly scale-dependent coefficient $C(\Delta)$, and using the approximation $\langle |\bar{S}|^3 \rangle \simeq \langle |\bar{S}|^2 \rangle^{\frac{3}{2}}$, one obtains

$$\epsilon = C(\Delta) 2^{3/2} \Delta^2 \langle \bar{S}_{ij}^2 \rangle^{3/2} + 2\nu \langle \bar{S}_{ij}^2 \rangle , \tag{5}$$

The moment $\langle \bar{S}_{ij}^2 \rangle \equiv \langle \bar{S}_{ij} \bar{S}_{ij} \rangle$ can be evaluated from the energy spectrum of the resolved field, which is assumed here to follow the Pao spectrum up to a sharp cutoff wavenumber $k_\Delta = \pi/\Delta$. The Pao spectrum, given by

$$E(k) = c_K \epsilon^{2/3} k^{-5/3} \exp\left(-\frac{3}{2} c_k k^{-4/3} \right)$$

is one of the cases considered by Voke (1996), and we use it here because resulting expressions are simple. Solving for C, one obtains

$$C(\Delta/\eta) = e^{-\frac{3}{2} c_K (\pi\eta/\Delta)^{4/3}} \left(\frac{\eta}{\Delta} \right)^2 \left(1 - e^{-\frac{3}{2} c_K (\pi\eta/\Delta)^{4/3}} \right)^{-3/2} . \tag{6}$$

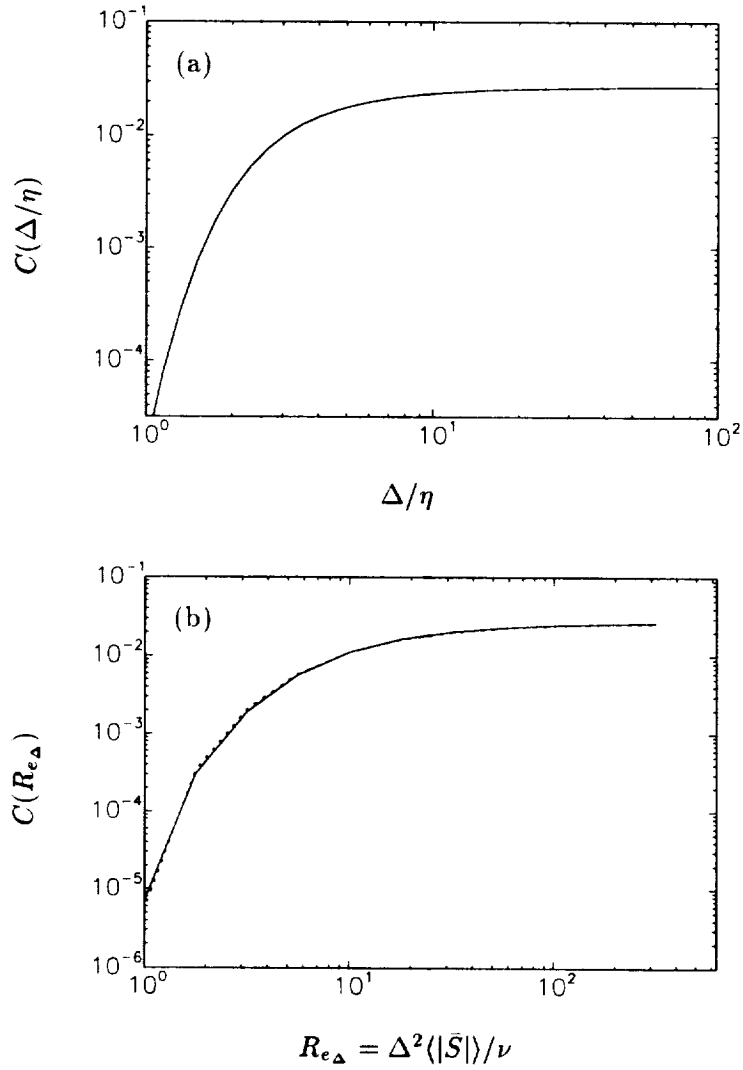

FIGURE 1. (a) Smagorinsky coefficient as calculated from the dissipation balance using the Pao spectrum (Eq. 6). (b) Same result but expressed in terms of mesh Reynolds number (solid line), obtained by solving Eq. 7. (see also Voke (1996), who expresses the same result in terms of the ratio of eddy to molecular viscosity). The dotted line is a convenient fit, namely $C_{\rm fit}(Re_\Delta) = 0.027 \times 10^{-3.23 Re_\Delta^{-0.92}}$.

The predicted variation in C is shown in Fig. 1a (for $c_K = 1.6$). As expected, the above estimate shows a rapid decrease in C as the grid-scale approaches the Kolmogorov scale.

For future reference, it is also useful to express the coefficient in terms of the mesh-Reynolds number $Re_\Delta = \Delta^2|\bar{S}|/\nu$ which (as opposed to Δ/η) is a variable that can be computed locally in LES. Using $\eta = (\nu^3/\epsilon)^{1/4}$ and replacing ϵ with the

r.h.s. of Eq. 5, one obtains

$$C(Re_\Delta) = \frac{\sinh^{-\frac{3}{2}}\gamma}{2^{\frac{3}{2}} Re_\Delta^{\frac{3}{2}} \sqrt{C(Re_\Delta) + Re_\Delta^{-1}}}\, e^{-\gamma/2}, \tag{7}$$

where

$$\gamma = \frac{3}{4} c_K \pi^{\frac{4}{3}} Re_\Delta^{-1} (C(Re_\Delta) + Re_\Delta^{-1})^{-\frac{1}{3}}.$$

In deriving this result it has been assumed that $\langle |\bar{S}| \rangle \simeq \langle |\bar{S}|^2 \rangle^{\frac{1}{2}}$. Solving for $C(Re_\Delta)$ numerically ($c_K = 1.6$) one obtains the curve shown in Fig. 1b. This curve is not too different from the empirically obtained result of McMillan & Ferziger (1979).

While the precise nature of these curves depends strongly on the assumed Pao spectrum, which is not entirely realistic, the general trend is quite robust: The coefficient begins to drop from the asymptotic value starting from scales significantly greater than the Kolmogorov scale. Evidently, at the transition between inertial and viscous range, the assumption that C does not depend on scale is not accurate.

3. A priori tests

The aim of this section is to evaluate Smagorinsky coefficients computed with the dynamic model operating on filtered DNS data of forced isotropic turbulence. The dynamic coefficient is then compared with the 'real' coefficient obtained by requiring that the model dissipate the correct amount of energy. Velocity fields at microscale Reynolds number $R_\lambda = 85$ were generated with the pseudo-spectral code of Rogallo (1981) on a 256^3 mesh. This data base has a very well-resolved dissipation range and was used previously by Lund and Rogers (1994) in their study of the topology of dissipative motions. This feature is important for the present study since we are interested in the behavior near the Kolmogorov scale. The maximum wavenumber scaled in Kolmogorov units is $k_{max}\eta = 3$, which corresponds to a mesh spacing of $\Delta_m = 3/\pi\eta \simeq 1\eta$.

From the DNS, we evaluate the coefficient from the large-scale portion of the spectrum using the dynamic model (Eq. 1), assuming that $C(\Delta) = C(\alpha\Delta)$. The analysis is repeated at various filtering scales Δ (cutoff wavenumbers π/Δ) and several values of α. For comparison, the coefficient can be obtained from the condition that the model dissipates the proper amount of energy,

$$C(\Delta) = -\frac{\langle \tau_{ij} \bar{S}_{ij} \rangle}{\Delta^2 2^{3/2} \left\langle (\bar{S}_{ij}^2)^{\frac{3}{2}} \right\rangle}. \tag{8}$$

Results are shown in Fig. 2. As can be seen, the 'real' coefficient is near $C \simeq 0.02 \rightarrow 0.04$ when $\Delta > 30\eta$, i.e. for scales above the viscous range. At smaller Δ, the coefficient decreases rapidly, qualitatively in accord with the theoretical prediction based on the Pao spectrum (Fig. 1a). We do not ascribe much significance to the discrepancies between Fig.1a and 2 since we have verified that they are due to minor differences between the Pao and the actual spectrum, and also due to

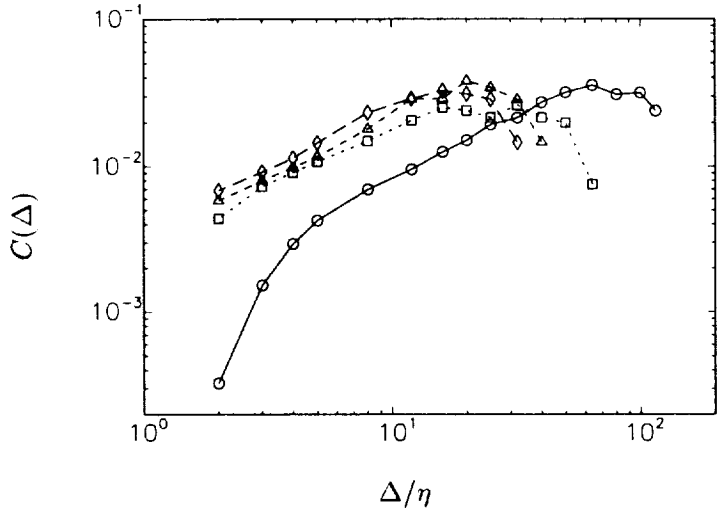

FIGURE 2. Coefficients obtained from *a priori* tests using well resolved DNS (256^3 simulation at $R_\lambda \simeq 85$ and $k_{max}\eta \simeq 3$). ○ , 'true coefficient' obtained from dissipation balance (Eq. 8). Other symbols: dynamic model coefficient (standard formulation) at various test-filters: □ , $\alpha = 2$; △ , $\alpha = 3$; ◇ , $\alpha = 4$.

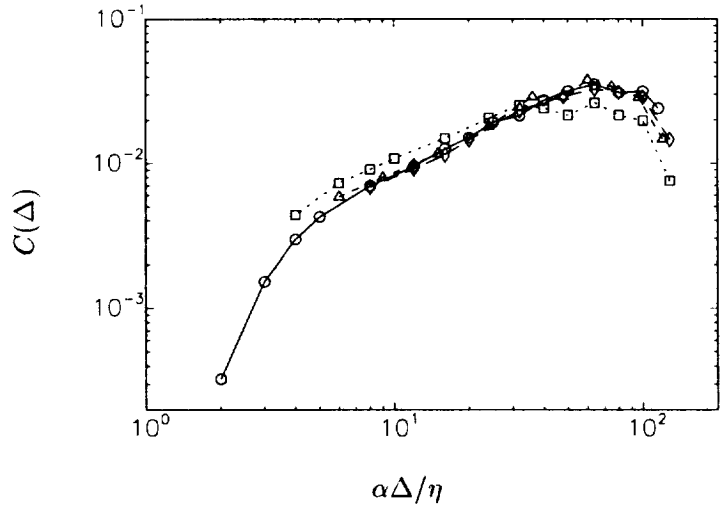

FIGURE 3. Same as Fig. 2, but plotted as function of $\alpha\Delta/\eta$. The near collapse means that the dynamic model yields the coefficient appropriate to the test-filter scale instead of the grid-scale.

residual unsteadiness in the simulations due to a limited sampling of velocity fields in time. At large scales a drop in coefficient can be seen, probably due to the effects of forcing.

The dynamic model predictions yield a similar trend for the coefficient, only that

the scale range appears to be shifted. Since the dynamic model samples the scales at the test-filter level, it is reasonable to expect that the resulting coefficient is the one corresponding to the test-filter scale instead of that of the grid-scale. To verify this idea, in Fig. 3 we plot the results of the dynamic model as function of the respective test-filter scales instead of the grid-scale (except for the coefficient obtained from Eq. 8). The collapse is quite good, indeed verifying that in this case the dynamic model yields the coefficient corresponding to the test-filter scale.

Similar results were obtained when using the strain-rate contraction (Germano *et al.*, 1991) for the dynamic model (for which $C = \langle L_{ij}\bar{S}_{ij}\rangle / \langle M_{ij}\bar{S}_{ij}\rangle$), or the least-square error approach to determine the 'real' coefficient (for which $C = -\langle \tau_{ij}|\bar{S}|\bar{S}_{ij}\rangle / 2\Delta^2 \langle |\bar{S}|^2\bar{S}_{ij}^2\rangle$). Therefore, the results are quite robust with regard to how the coefficients are determined.

At this point we conclude that the dynamic model is capable of reproducing the important trend that the coefficient should decrease as the filter-length approaches the Kolmogorov scale. Nevertheless, some discrepancy is observed between the 'real' and dynamic coefficient for scales at which the coefficient is strongly scale-dependent. From a practical perspective, this discrepancy is quite benign in the current application, since the dominant mechanism of energy drain when the filter is near the Kolmogorov scale is the resolved viscous dissipation. Indeed, simulations with resolutions in the viscous range run with the dynamically obtained coefficient (which according to Fig. 2 may be too high) did not show any significant difference from one using a lower coefficient, essentially because the SGS dissipation is negligible in these cases.

In what follows, we examine several reformulations of the dynamic model that attempt to explicitly include the scale-dependence of the coefficient. Because it affords relative ease of implementation and interpretation, the analysis is still conducted within the context of the viscous range, even though the impact of using different values for the coefficients is rather small.

4. Alternative formulations

In this section, we consider several alternative formulations of the dynamic model. None of the options considered will be found to be completely satisfactory, but the observations made along the way provide useful insights into the workings of the dynamic model.

4.1 The limit $\alpha \to 1$

Since we have found that (for $\alpha \geq 2$) the standard dynamic model yields the coefficient $C(\alpha\Delta)$ instead of $C(\Delta)$, an obvious possible remedy would be to allow the test filter scale to approach the grid scale. This issue was briefly addressed theoretically by Gao & O'Brien (1993), who noticed that while the resulting expressions would be indeterminate, the limit may be written in terms of higher-order gradients of the resolved velocity, thus emphasizing the scales closest to the grid-scale. A possible disadvantage of this approach is that the scales closest to the cutoff are often strongly affected by numerical errors.

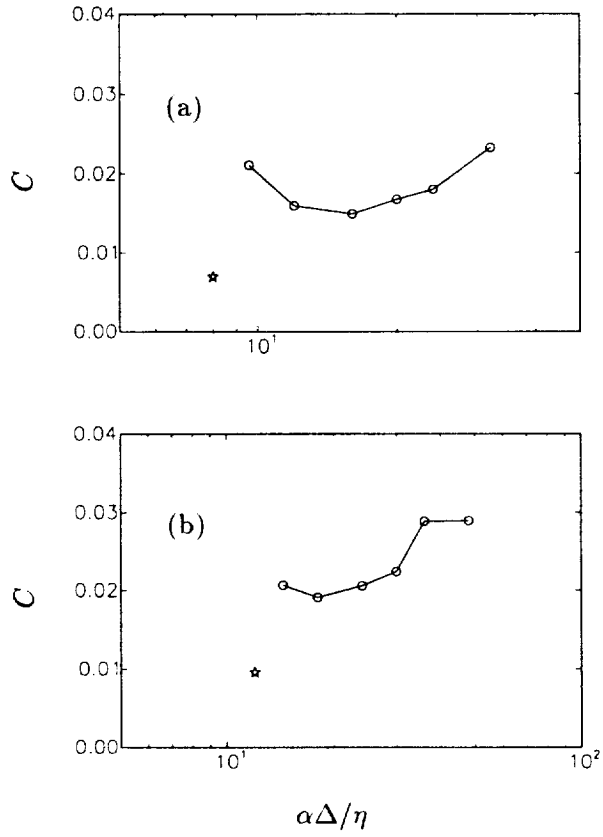

FIGURE 4. o , Coefficients obtained from the dynamic model at different test-filtering scales (from right to left, $\alpha = 4, 3, 2.5, 2, 1.5$ and 1.3). $\star$, Coefficient value obtained from dissipation balance (Eq. 8) at the grid scale (a) Grid-scale is $\Delta = 8\eta$, (b) Grid-scale is $\Delta = 12\eta$.

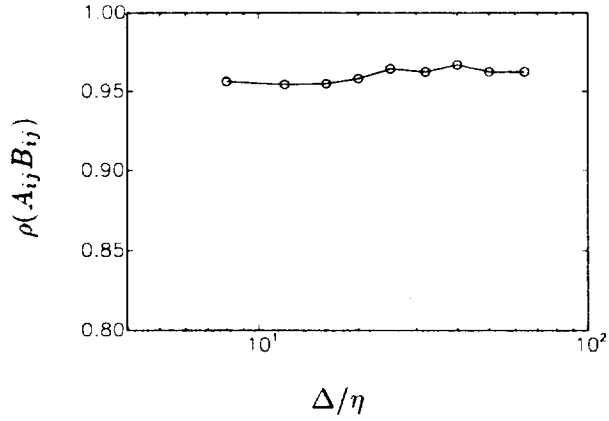

FIGURE 5. Correlation coefficient between the model tensors A_{ij} and B_{ij} measured from filtered DNS as function of filter scale. The correlation coefficient is computed according to $\rho(A, B) = \langle A_{ij} B_{ij} \rangle / \sqrt{\langle A_{ij}^2 \rangle \langle B_{ij}^2 \rangle}$.

To see if the limit $\alpha \to 1$ can be used to advantage in this case, we repeat the *a priori* test of the previous section and compute the dynamic model coefficient at the smaller filter-width ratios of $\alpha = 1.5$ and $\alpha = 1.3$. Figure 4a shows the results for a grid-scale $\Delta = 8\eta$, and 4b for $\Delta = 12\eta$. In both cases, it is apparent that for $\alpha \geq 2$ there is a smooth trend of the dynamic coefficient tending towards the 'true' coefficient as obtained from the dissipation balance. However, for $\alpha < 2$, there is a change in behavior and the coefficient increases again and does not tend towards the expected value as $\alpha \to 1$. While such a result may be specific to present conditions of analysis, it suggests that as the width of the band between grid and test filter becomes small, the procedure can yield unphysical results. For this reason, we do not consider this approach further.

Before proceeding however, we notice from Fig. 4 that for $\alpha > 2$ the approach towards the 'true' coefficient appears to be exponential. This observation will be used in §4.3.

4.2 Solving for two coefficients

Here we return to the case $\alpha = 2$. Instead of assuming that $C(\Delta) = C(2\Delta)$, we investigate the proposal of Moin & Jiménez, (1993) where the least-square-error approach is used to solve for the two coefficients. Upon solving the linear set of equations, one obtains (using, say, volume averaging)

$$C(\Delta) = \frac{\langle A_{ij}L_{ij}\rangle \langle B_{ij}^2\rangle - \langle B_{ij}L_{ij}\rangle \langle A_{ij}B_{ij}\rangle}{\langle A_{ij}^2\rangle \langle B_{ij}^2\rangle - \langle A_{ij}B_{ij}\rangle^2}, \tag{9a}$$

$$C(2\Delta) = \frac{\langle A_{ij}L_{ij}\rangle \langle A_{ij}B_{ij}\rangle - \langle B_{ij}L_{ij}\rangle \langle A_{ij}^2\rangle}{\langle A_{ij}^2\rangle \langle B_{ij}^2\rangle - \langle A_{ij}B_{ij}\rangle^2}. \tag{9b}$$

The averages can be evaluated from the DNS (as in §3) at different scales, and the coefficients computed from the above expressions. However, the results appear to be unphysical: both $C(\Delta)$ and $C(2\Delta)$ were found to be negative, with large scatter from one scale to another.

The cause for this problem can be traced to the fact that the two tensors A_{ij} and B_{ij} (or $\alpha^2|\hat{\tilde{S}}|\hat{\tilde{S}}_{ij}$ and $|\widehat{\tilde{S}}|\widehat{\tilde{S}}_{ij}$) are strongly correlated. The correlation coefficient between them is evaluated from the DNS and plotted in Fig. 5, for different scales. Due to the strong tensor-alignment, the system of equations is ill conditioned. It is interesting to point out that in the standard dynamic model, the coefficient is determined mainly by the fact that both tensors have significantly different magnitudes (due to the coefficient α^2). However, to use additional (directional) information from the Germano identity, at least in the context of the Smagorinsky model, appears not feasible.

4.3 The bi-dynamic model

This version of the dynamic model is motivated by our observation that the model provides the coefficient at the test-filter level $\alpha\Delta$. While this suggested taking the

limit $\alpha \to 1$, it was shown in §4.1 that then the Germano identity relied on less and less modes between test and grid filter, modes that are often most affected by numerical errors. Another alternative formulation is to compute coefficients from two different test filters and use these to extrapolate to the grid scale. Briefly, one assumes that the dynamic coefficient obtained by the traditional method (with M_{ij} given by Eq. 2) is a smooth function of the test-to-grid filter ratio α. In fact, noting the exponential behavior in Figs. 4 for $\alpha > 2$, it is more convenient to write that C is a smooth function of β, where $\alpha\Delta = 2^{\beta}\Delta$. The usual case $\alpha = 2$ corresponds to $\beta = 1$, while the limit $\alpha \to 1$ is obtained as $\beta \to 0$. Let us therefore denote the coefficient obtained from the traditional method as $C(\beta)$. Next, we expand $C(\beta)$ in Taylor series around $\beta = 1$,

$$C(\beta) = C(\beta = 1) + \frac{dC}{d\beta}|_1(\beta - 1). \tag{10}$$

To evaluate $dC/d\beta$ we introduce a secondary test-filter at scale, say, 4Δ ($\beta = 2$), evaluate the corresponding coefficient $C(\beta = 2)$, and compute the coefficient derivative using one-sided finite-difference, $(dC/d\beta)|_1 \simeq C(2) - C(1)$. The information employed has been obtained at and above scale 2Δ, where according to the results of §4.1 robust results can be expected. Since we are interested in the limit $\beta \to 0$, we now propose to simply evaluate Eq. 10 at $\beta = 0$. The resulting coefficient can be written as follows:

$$C = 2\frac{\langle M_{ij}L_{ij}\rangle}{\langle M_{ij}M_{ij}\rangle} - \frac{\langle N_{ij}F_{ij}\rangle}{\langle N_{ij}N_{ij}\rangle}, \tag{11}$$

where the tensors F_{ij} and N_{ij} are defined exactly as the tensors L_{ij} and M_{ij} respectively, only using a test-filter scale equal to 4Δ instead of 2Δ.

This basic formulation is first tested *a priori*: The DNS data is filtered at an additional test-filter scale to compute F_{ij} and N_{ij}. The coefficient C is evaluated according to Eq. 11 using volume averaging, and the analysis is repeated at several grid-scales Δ. Figure 6 shows the results. As can be seen, the 'bi-dynamic' model is very noisy since it is based on extrapolation. Nevertheless, the procedure does improve the prediction of the standard dynamic model. Importantly, this approach preserves the basic foundation of the dynamic model which only uses information from the resolved scales, instead of relying on equilibrium arguments to calibrate the coefficient and its dependence on scale.

The approach is implemented in LES of forced isotropic turbulence on 32^3 modes. The code and methodology is the same as that described in Meneveau *et al.* (1996), but using volume averaging. The primary and secondary test-filtering are performed using cutoff filters at scales 2Δ and 4Δ, and 14 simulations are run with various viscosities to vary the mean mesh Reynolds number. The results are shown in Fig. 7, where the volume averaged terms $C(1) = \langle LM\rangle / \langle MM\rangle$, $C(2) = \langle FN\rangle / \langle NN\rangle$ and the extrapolated result $C(0) = 2\langle LM\rangle / \langle MM\rangle - \langle FN\rangle / \langle NN\rangle$ are shown. The latter coefficient is used in the subgrid model. As can be seen, the results appear to display the correct trend, although some features are noteworthy: At

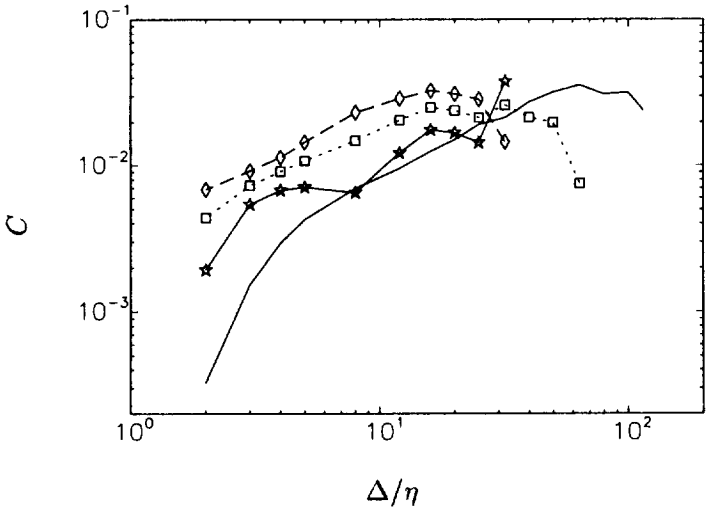

FIGURE 6. *A priori* test of extrapolation procedure, based on DNS results described in Fig. 2. ——— , 'Real' coefficients from dissipation balance; ◇ and □ , Dynamic coefficients at $\alpha = 4$ and $\alpha = 2$; ⋆, extrapolated values according to Eq. 11.

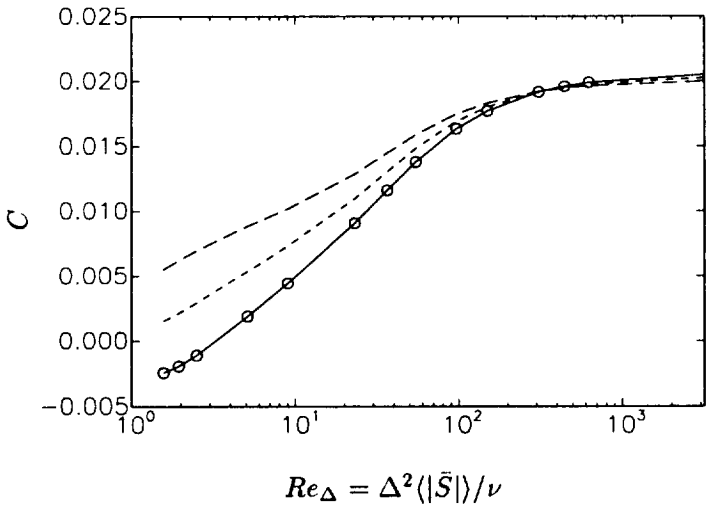

FIGURE 7. Coefficients obtained in LES of forced isotropic turbulence at various Reynolds numbers, using the bi-dynamic model with volume averaging. ——— , Value at scale 4Δ, $\langle FN\rangle / \langle NN\rangle$; ---- , Value at scale 2Δ, $\langle LM\rangle / \langle MM\rangle$; ○ , 'Bi-dynamic' coefficient obtained by extrapolation to scale Δ, $2\langle LM\rangle / \langle MM\rangle - \langle FN\rangle / \langle NN\rangle$. This coefficient is used in the LES. As reference, the Taylor-microscale Reynolds number $R_\lambda = \sqrt{15u'^4/(\nu\epsilon)}$ (where ϵ is the total dissipation) ranges from $R_\lambda = 17$ to $R_\lambda = 2,300$.

large Reynolds numbers, the coefficient value asymptotes to a slightly smaller value than the standard dynamic model. No simple explanation for this trend has been found.

Qualitatively, one expects the model to be quite stable because if, say, $C(\beta = 1)$ falls below its appropriate value while $C(\beta = 2)$ remains fixed, the extrapolated coefficient will drop significantly. This will cause more 'pile-up' of energy near the grid-scale, raising the value of $C(1)$ and raising the extrapolated coefficient. This in turn damps the smallest scales. The opposite occurs if $C(1)$ is initially increased, with excessive damping causing $C(1)$ to diminish. However, the equilibrium point of this version of the model appears to establish itself at a slightly smaller value than that of the traditional approach, even at very large Reynolds numbers where viscosity does not affect the results. Another observation is that at very small Re_Δ, the extrapolation process yielded negative coefficients. This is essentially an extrapolation error. In this application, this error had no impact on the simulation due to the smallness of the SGS term at such low mesh Reynolds numbers.

Finally, an attempt was made to replace the volume averaging with Lagrangian averaging (Meneveau *et al.*, 1996). The motivation is to enable applications of the dynamic model to LES of complex-geometry flows, where no directions of statistical homogeneity exist, but where some averaging must still be performed. In the 'Lagrangian bi-dynamic model', one would compute four variables $\mathcal{I}_{LM}$, $\mathcal{I}_{MM}$, $\mathcal{I}_{FN}$, and $\mathcal{I}_{NN}$, which correspond to the pathline averages of the source terms $L_{ij}M_{ij}$, M_{ij}^2, $F_{ij}N_{ij}$ and N_{ij}^2 respectively. They are obtained by integrating relaxation transport equations with a prescribed relaxation time-scale (Meneveau *et al.*, 1996). To be consistent with this reference, we must choose two relaxation time-scales, $T_1 = 1.5\Delta(\mathcal{I}_{LM}\mathcal{I}_{MM})^{-1/8}$ and $T_2 = 1.5\Delta(\mathcal{I}_{FN}\mathcal{I}_{NN})^{-1/8}$. T_1 is used in the equations for $\mathcal{I}_{LM}$ and $\mathcal{I}_{MM}$, while T_2 is used for $\mathcal{I}_{FN}$ and $\mathcal{I}_{NN}$. With these time-scales it is assured that the numerators $\mathcal{I}_{LM}$ and $\mathcal{I}_{FN}$ never become negative. Then, the coefficient at the grid-scale is computed by extrapolation at every point according to $C(0) = 2\mathcal{I}_{LM}/\mathcal{I}_{MM} - \mathcal{I}_{FN}/\mathcal{I}_{NN}$.

Overall, this approach resulted in several difficulties due to the spatial variability of the local coefficient coupled with the extrapolation procedure. Even though the method guarantees the individual coefficients at the two test-filter levels to be positive, there were many instances in which $\mathcal{I}_{FN}/\mathcal{I}_{NN} > 2\mathcal{I}_{LM}/\mathcal{I}_{MM}$, and therefore the extrapolated coefficient was negative causing instability or unphysical results.

To stabilize the simulation it was necessary to perform an additional pathline averaging of the coefficient $C(0)$ itself, with an appropriately selected relaxation time-scale so that it would not become negative. Denoting the Lagrangian average of the coefficient by $\mathcal{I}_C$, the time-scale chosen was $T_3 = 1.5\Delta[(\mathcal{I}_C\mathcal{I}_{MM})\mathcal{I}_{MM}]^{-1/8}$. On average, this time-scale is of the same order as T_1 and T_2. Results are shown in Fig. 8. The average of the coefficient shows the appropriate trend, although the extrapolated coefficient is not much smaller than the value at scale 2Δ, and at low Re_Δ is considerably higher than the expected values (compare with Fig. 5). Given the extra expense (carrying five relaxation-transport equations instead of two) and

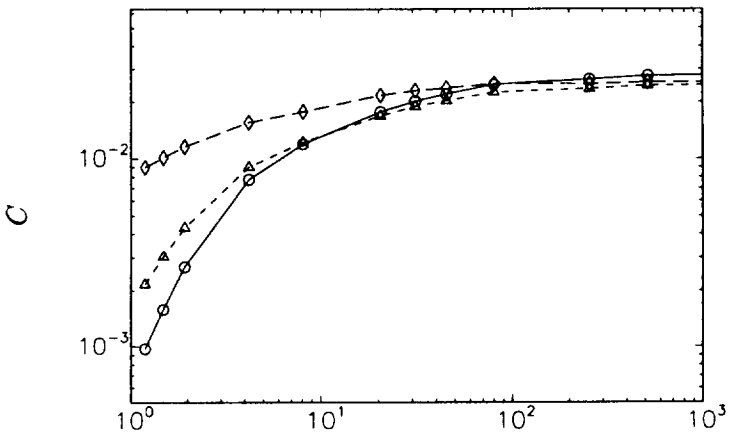

FIGURE 8. Coefficients obtained during LES of forced isotropic turbulence at various Reynolds numbers, using the bi-dynamic model with Lagrangian averaging of numerators and denominators, and additional averaging of extrapolated coefficient. Shown is the volume average of the coefficient (which varies locally). $\diamond$, Value at scale 4Δ, $\langle \mathcal{I}_{FN}/\mathcal{I}_{NN}\rangle$; $\triangle$, Value at scale 2Δ, $\langle \mathcal{I}_{LM}/\mathcal{I}_{MM}\rangle$. o , Mean 'bi-dynamic coefficient' obtained by extrapolation to scale Δ.

the small improvement, this approach does not seem to constitute a method of choice.

4.4 Using non-dynamic estimates for scale-dependency

A more robust method is to explicitly build scale-dependence into the dynamic model. This is accomplished by rewriting Eq. 1 (for $\alpha = 2$) as follows

$$L_{ij} = C(\Delta)\left(\frac{C(2\Delta)}{C(\Delta)}A_{ij} - \hat{B}_{ij}\right), \tag{12}$$

and solve for $C(\Delta)$ as in Eq. 2, but with M_{ij} given by

$$M_{ij} = f(\Delta)A_{ij} - B_{ij}, \tag{13}$$

where

$$f(\Delta) = \frac{C(2\Delta)}{C(\Delta)}.$$

The idea is to solve for the coefficient $C(\Delta)$ but to use prior knowledge about the possible scale dependence to evaluate the function $f(\Delta)$. In the present case of approaching the viscous range, this function depends on the dimensionless parameters Δ/η or Re_Δ. As mentioned previously, the latter case is more convenient during LES since it is based on the strain-rate magnitude, which may be evaluated locally.

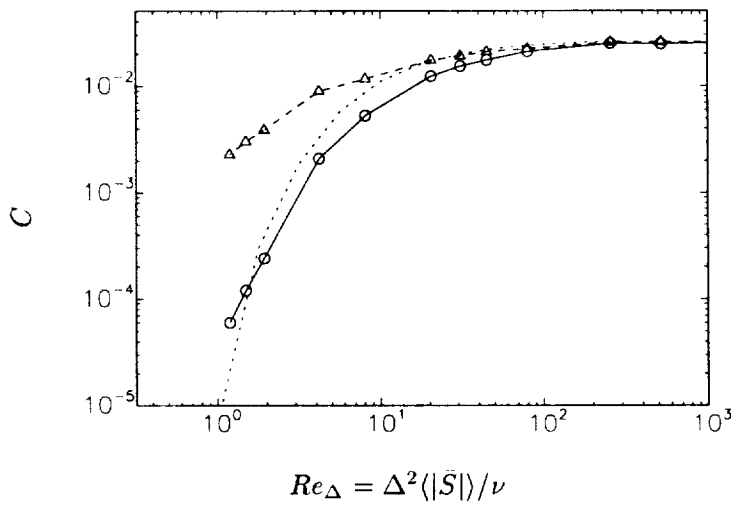

FIGURE 9. Coefficients obtained in LES of forced isotropic turbulence, using the Lagrangian dynamic model in which scale dependence is incorporated non-dynamically. Shown are the mean values of the coefficients. Average mesh Reynolds number is varied systematically by changing ν. $\triangle$, mean coefficient using standard formulation, Eq. 2 and 2a; o , modified dynamic model, in which M_{ij} is given by Eq. 11; ---- , prediction based on Pao spectrum (Eq. 7).

Using Eq. 7, we evaluate the ratio $C(2\Delta)/C(\Delta)$, which can be fitted quite well by the following expression:

$$f(Re_\Delta) = 10^{-3.23[Re_{2\Delta}^{-0.92} - Re_\Delta^{-0.92}]}, \tag{14}$$

where $Re_{2\Delta} = 4\Delta^2|\hat{\bar{S}}|/\nu$. When the mesh Reynolds number is evaluated based on the local strain-rate magnitude, it may locally approach zero. Then Eq. 14 diverges, which can cause numerical difficulties. Thus, the expression is clipped at $f(Re_\Delta) = \max[f(Re_\Delta), 100]$. This approach was tested *a priori* and gave good results in the sense that the coefficient obtained by this modified method is indeed smaller than the value that would have been obtained by assuming $C(\Delta) = C(2\Delta)$.

The approach was then implemented in LES of forced isotropic turbulence on 32^3 modes using the Lagrangian method of averaging (Meneveau *et al.*, 1996), accumulating two variables $\mathcal{I}_{LM}$ and $\mathcal{I}_{MM}$ instead of five as in §4.3. The code and methodology was the same as that described in the above reference, except for the definition of M_{ij}. The local values of M_{ij} were computed from Eq. 13, and the local mesh Reynolds number Re_Δ was based on the local strain-rate magnitude. In order to span a significant range of Re_Δ, 14 simulations with different values of ν were carried out. For comparison, simulations were also done with the standard definition of M_{ij}, i.e. assuming that $C(\Delta) = C(2\Delta)$. Results are shown in Fig. 9 as function of the average value of the cell Reynolds number. Each symbol represents the result of a simulation that was run to a statistically stationary state. For comparison, the

dotted line shows the theoretical prediction of Eq. 7. As can be seen, the approach provides improved prediction of the coefficient compared to the standard dynamic model. As stated before, the difference in coefficient had no appreciable effect on the resolved scales or their energy spectrum.

This approach provides robust predictions of the coefficient for this case (in the viscous range), and is very easy to implement. However, it requires input based on theoretical arguments. It can thus only be applied to cases in which one knows *a priori* the dependence of the ratio of coefficient on scale. Therefore, this approach is not entirely dynamic, in the sense that important information about model coefficients must be specified and is not determined during the simulation.

5. Conclusions

The dynamic Smagorinsky model has been examined in a case where it is known *a priori* that the coefficient depends on scale, namely in the viscous range. Theoretical arguments were reviewed giving the coefficient's expected dependence on scale or on mesh Reynolds number. *A priori* tests using well-resolved DNS data revealed an important property of the standard dynamic model as applied to such a case: The method gives the coefficient corresponding to the test-filter scale instead of the grid-scale.

Several possible reformulations of the dynamic model were examined and/or tested in LES of isotropic turbulence. In the first, the limit $\alpha \to 1$ was considered. Using *a priori* tests at test-filter scales near the grid scale ($\alpha = 1.5$ and 1.3), it was shown that unphysical behavior can result. This limit is also expected to be susceptible to numerical errors. Another proposal was studied in which the Germano identity is used to solve for two unknown coefficients $C(\Delta)$ and $C(2\Delta)$ in the least-square-error sense. For implementations with the Smagorinsky model, this procedure was shown to be ill-conditioned essentially because the eigenvectors of the two basis tensors $|\hat{\bar{S}}|\hat{\bar{S}}_{ij}$ and $\widehat{|\bar{S}|\bar{S}_{ij}}$ are almost 'co-linear' (their correlation coefficient is about $\rho \simeq 0.96$).

A new procedure, the bi-dynamic model, was proposed and tested. It is based on extrapolating coefficients obtained at two test-filters. When implemented with volume averaging, the method gave fair results. Some complications arose when the method was coupled with Lagrangian averaging. We conclude that while the idea of using more than one test-filter scale to sample the resolved field in more detail appears to be promising in principle, in the present application the added complications outweigh the benefits. Finally, we tested a modified formulation in which one solves for a single coefficient at the grid-scale but must prescribe the ratio of coefficients at test and grid scales non-dynamically. This method proved quite practical, and it gave good results. However, it is not completely dynamic since prior theoretical information about scale-dependence must be employed (a similar approach was employed to account for grid anisotropy in Scotti *et al.*–in this volume).

Acknowledgments

This work profited from fruitful discussions with Prof. P. Moin. The financial support of CTR and ONR (N00014-92-J-1109, monitored by Dr. P. Purtell) is gratefully acknowledged.

REFERENCES

BARDINA, J., FERZIGER, J. H., & REYNOLDS, W. C. 1980 Improved subgrid scale models for large eddy simulation. *AIAA-80-1357.*

LILLY, D. K. 1967 The representation of small-scale turbulence in numerical simulation experiments. In *Proc. IBM Scientific Computing Symposium on Environmental Sciences.*

LIU, S., MENEVEAU, C., & KATZ, J. 1994 On the properties of similarity subgrid-scale models as deduced from measurements in a turbulent jet. *J. Fluid Mech.* **275,** 83-119.

LIU, S., MENEVEAU, C., & KATZ, J. 1995 Experimental study of similarity subgrid-scale models of turbulence in the far-field of a jet. *Appl. Sci. Res.* **54,** 177.

LUND, T. S. & ROGERS, M. M. 1994 An improved measure of strain state probability in turbulent flows. *Phys. Fluids.* **6,** 1838-1847.

MCMILLAN, O. J. & FERZIGER, J. 1979 Direct testing of subgrid-scale models. *AIAA-79-0072.*

MENEVEAU, C., LUND, T. S., & CABOT, W. H. 1996 A Lagrangian dynamic subgrid-scale model of turbulence. *J. Fluid Mech.* **319,** 353.

MOIN, P. & JIMÉNEZ, J. 1993 Large Eddy Simulation of Complex Turbulent Flows. *AIAA-93-3099.*

VOKE, P. R. 1996 Subgrid-scale modeling at low mesh Reynolds number. *Theor. Comp. Fluid Dyn.* **8,** 131-143.

ROGALLO, R. S. 1981 Numerical experiments in homogeneous turbulence. NASA Tech. Memo. 81315, NASA Ames Research Center.

ZANG, Y., STREET, R. L., & KOSEFF, J. 1993 A dynamic mixed subgrid-scale model and its application to turbulent recirculating flows. *Phys. Fluids A.* **5,** 3186-3196.